The segmental and rotational dynamics of PPO, above the glass-transition, investigated by Neutron Scattering and Molecular Dynamics simulations

C. Tengroth[1], D. Engberg[1], P. Carlsson[2], P. Ahlström[3], G. Wahnström[1], W.S. Howells[4], L. Börjesson[1]

[1] Department of Applied Physics
Chalmers University of Technology and Göteborg University, SE-412 96 Göteborg, Sweden

[2] Department of Experimental Physics
Chalmers University of Technology and Göteborg University, SE-412 96 Göteborg, Sweden

[3] School of Engineering, University College of Borås, S-501 90 Borås, Sweden

[4] Rutherford Appleton Laboratory, Chilton, OX11 0QX, UK

April 17, 2005

Abstract

The relaxation properties of poly(propylene oxide) at temperatures above the glass-transition are studied by quasi-elastic neutron scattering and Molecular Dynamics simulations. The contributions to the dynamic structure factor from the segmental motion and the methyl group jump rotation are separated using a threefold jump-rotation model for the methyl side group motion, with a delta function for the distribution of relaxation times, and a stretched exponential function for the segmental motion.

This simple model describes momentum transfer and time dependence of the data well over a wide temperature range. The results show that with this separation both neutron and MD data can be well described and the analysis of both contributions is necessary in

order to obtain reliable results for the segmental relaxation and rotational relaxation times at temperature above T_g

1 Introduction

There has been a considerable effort in recent years towards the understanding of relaxational processes in polymers above and below the glass-transition temperature T_g. This interest partly arose due to the success of recent theories to describe some characteristic features concerning the rapid slowing down of dynamics in the supercooled liquid close to T_g.

For polymeric glass-formers it is the segmental motion that is associated with the structural arrest at the glass-transition. Quasi-elastic neutron scattering (QENS) is an important tool, for the experimental studies of the rotational and segmental relaxation not only for the high incoherent scattering cross-section of hydrogen, but also because QENS gives spatial information about the observed dynamics on a length scale equivalent to the distance between monomers.

In the past, studies on the segmental motion were concentrated on polymers with no side chains at temperature high enough for the segmental motion to dominate or made on polymers with deuterated rotational groups not to detect them. [1, 2, 3, 4, 5, 6, 7] There has also been a large interest in methyl group motions in polymers, [8, 9, 10, 11, 12] not least to explain the quantum mechanical tunnelling in disordered matter[13]. These studies have lead to considerable insight into the side-group motion, but are often performed at low enough temperatures or on selectively deuterated polymers in order make it possible to disregard the segmental motion.

At temperatures where several different types of motions are present the highly complicated structure and dynamics of an amorphous polymer with a large variety of chain conformations calls for computer modelling to unravel the detailed microscopic structure and dynamics. Recently, MD simulations have been employed in conjunction with neutron scattering and NMR to study the motion of CH_3 groups also above the glass-transition. [14, 15] The time and spatial range of the motion of interest is also very appropriate for Molecular Dynamics (MD) simulations.

In order to investigate the segmental motion and the methyl group rotation we have made a combined QENS and MD study of the highly flexible poly(propylene oxide). Previously Reverse Monte Carlo (RMC) modelling was used to investigate the structure of, PPO[16]. Then, using the RMC model as a starting structure, the forcefield proposed in Ref. [17] was successfully used in Ref. [18] to describe the structure of PPO. The results

compared even more favourably with the experimental structure factor when a quantum path-integral approach was used.[19] We here use the same force field, but extend the study to concern also dynamic properties, together with a report on an incoherent QENS study of the relaxational dynamics in PPO over a wide temperature range, above T_g.

We show that for the QENS experiment and the MD simulation the methyl group rotation and the segmental motion in hydrogenous PPO can be separated using a simple model and assuming that the two processes are decoupled. The approach is shown to give physically realistic results for both kinds of motions and demonstrates the importance to model both motions to be able to achieve coherent results, for polymers with side chains. At temperatures where the segmental motion is appreciable one can remove the signal from the $-CH_3$ groups by deuterating them and thereby only study the segmental motion. It is however not possible to study only the rotations by deuterating the matrix, since the motion of the $-CH_3$ group will be a convolution of segmental and rotational motion. Both motion types have to be taken into account to get consistent results. The results of a first attempt to use the model for PPO data in a limited temperature range have been reported earlier.[20]

2 Experimental

2.1 Neutron Scattering

Poly(propylene oxide) (PPO), $T_g = 195$K, of average molecular weight $M_w \approx 4000$ and with a polydispersity of 1.05 was purchased from Polysciences. Light-weight impurities were removed from the polymer by freeze drying on a vacuum line. The neutron scattering experiments were carried out at the neutron spallation source ISIS, using the back-scattering spectrometer IRIS. The sample was placed in a flat aluminium can, 4x4 cm and 0.5 mm thick, at an angle 45° relative to the beam. Temperature control was achieved through a closed-cycle refrigerator (CCR). The analyser energy for the graphite array (PG002) was 1.84 meV, giving an energy resolution $\Delta E = 15$ μeV FWHM and a momentum transfer range of $0.45 < Q/\text{Å}^{-1} < 1.85$. The experimental data were corrected and converted to dynamic structure factors using on site programs. Multiple scattering was treated in the isotropic approximation. Data from detectors in the plane of the sample, suffered from severe self-scattering and were discarded. The scattering was normalised to the scattering from a vanadium plate. Spectra were recorded at temperatures ranging from 240 K up to 350 K.

In a neutron scattering experiment the measured intensity is proportional to the double-differential scattering cross section

$$\frac{\partial^2\sigma}{\partial\omega\partial\Omega} \propto \frac{k}{k_0}\{\sigma_{\rm coh}S_{\rm coh}(Q,\omega) + \sigma_{\rm inc}S_{\rm inc}(Q,\omega)\}, \quad (1)$$

where $S(Q,\omega)$ is the dynamic structure factor and the subscripts inc and coh denote the incoherent and coherent components. PPO mainly contains protons that have a large incoherent neutron scattering cross section ($\sim$ 80 barns) compared to their coherent part and to the other elements in the monomer ($\sim$ 5 barns). Therefore, in the neutron scattering experiment the observed dynamics mainly corresponds to the self-correlation function of the hydrogen nuclei.

2.2 Molecular Dynamics

The molecular weight used in the simulations was $M_w \approx 2000$ (45 repeat units + CH_3 terminations). This is less than used in the QENS experiment but previous studies [21] show no great change of the microscopical dynamics above ≈ 10 monomer units. Periodic boundary conditions were used and the number of molecules (atoms) were 21 (9639).

The system was generated using a random walk technique and subsequently adjusted to experimental data using the Reverse Monte Carlo technique. [16]. This was followed by a united atom simulation, [22] in which MD trajectories were generated for a nanosecond with, essentially, the GROMOS forcefield [23]. Then explicit H-atoms were added and the force field changed to the one defined in Ref.[17]. The system was equilibrated for 2 ns, with a weak coupling to a pressure reservoir the first 0.5 ns. This coupling was then slowly turned of. The production runs were run in a NVT-ensemble for 1 ns. All MD simulations were performed using the simulation package Gromacs [24] For further description of the simulation, see Ref.[18].

In Ref. [18], the 300 K run was used to study the structure of PPO. In this study we analyse the dynamic properties of that simulation and include two new runs at 240 K and 325 K.

3 Molecular Model

There is a multitude of different kinds of dynamics in a polymer. They can be divided into segmental, rotational and vibrational motions. Since the experiment was performed on a hydrogenous sample, mainly the incoherent (self) scattering of hydrogen is seen and accordingly only the self correlations

are analysed. The intermediate scattering function $S(Q,t)$ for a system where 3/6 of the H atoms (those in the methyl group) take part in the rotation and 3/6 of them (those on the main chain) do not, can, if we assume that they are decoupled, be written:

$$S^{\mathrm{mod}}(Q,t) = S^{\mathrm{seg}}(Q,t)\{\frac{3}{6} + \frac{3}{6}S^{\mathrm{rot}}(Q,t)\}S^{\mathrm{vib}}(Q,t) \tag{2}$$

Here S^{seg}, describes the segmental relaxations of the whole polymer, S^{rot} the rotational and librational motion of the CH_3 group and S^{vib} vibrations in the system. We do not consider the vibrations in this work, they will just be used as a Q-dependent pre-factor, including background and multiple-scattering effects, so from here on this factor is dropped.

Segmental relaxational processes in amorphous polymers are often described using a stretched exponential function, see Eq. 3, also known as the KWW-function. [10, 25, 26] The intermediate (self) structure factor is then described by the following expression;

$$S^{\mathrm{seg}}(Q,t) = \exp\{-(t/\tau_{\mathrm{seg}}(Q))^{\beta}\} \tag{3}$$

where $\tau_{\mathrm{seg}}(Q)$ is a Q dependent relaxation time, and β is the stretching parameter $0 < \beta \leq 1$. When assuming a power law dependence with the power ν this can be rewritten for convenience as

$$\tau_{\mathrm{seg}}(Q) = \tau_{\mathrm{seg}}(Q_0) \cdot (\frac{Q_0}{Q})^{\nu}, \tag{4}$$

where $\nu \in [0, \infty[$ and Q_0 is an (insignifcant) scaling parameter. The average relaxation time $\langle\tau_{\mathrm{seg}}(Q)\rangle$ is related to $\tau_{\mathrm{seg}}(Q)$ via

$$\langle\tau\rangle = \frac{\tau}{\beta}\Gamma(\frac{1}{\beta}) \tag{5}$$

where Γ denotes the gamma function. If $\beta = 1$ the single exponential function is recovered, with $\tau_{\mathrm{seg}}(Q) \propto Q^{-2}$ and Fickian diffusion is modelled. With $\tau_{\mathrm{seg}}(Q) \propto Q^{-4}$ a Rouse type of motion is described. A cross-over in the segmentational relaxation between Gaussian diffusion based on the Rouse model for the polymer chain, and Fickian diffusion is expected since the former is a consequence of chain diffusion while the latter describes local dynamics (cf., e.g., [27]).

The methyl group dynamics is represented by a three site jump rotation model [28] which has a Q-independent single exponential relaxation function.

$$S^{\mathrm{rot}}(Q,t) = A_0(Q) + \{1 - A_0(Q)\}\exp(-t/\tau_{\mathrm{rot}}) \tag{6}$$

Here $A_0(Q)$, the elastic incoherent structure factor (EISF), describes the Q-dependence of the methyl group motion. If all the CH_3 groups perform 120 degrees rotational jumps over three positions around the C-CH_3 bond, the EISF can be expressed analytically as: [28]

$$A_0(Q) = \frac{1}{3}(1 + 2j_0(\sqrt{3}Qr)) \tag{7}$$

with j_0 being the zeroth-order spherical Bessel function and r = 1.04 Å is the radius on which the hydrogen atoms of the methyl group are rotating.

At lower temperature, this might have to be extended to a model where a distribution of relaxation times is assumed as in e.g. Ref. [8, 12]. Alternatively a stretching parameter similar to the segmental motion can be used. Since, for PPO, the simple form of Eq. 6 is sufficient, as shown later in this report, we will not expand more on this issue here.

In MD one can directly study the dihedral angle, $\phi(t)$, defined either by CCCH or OCCH. We characterise the rotational motion by the following correlation function

$$C(t) = \frac{1}{N}\sum_i \langle \cos\{\phi_i(t) - \phi_i(0)\}\rangle \tag{8}$$

This can, if assumed decoupled, be further factorised into a rotational and a librational part

$$C(t) = C^{\mathrm{rot}}(t)C^{\mathrm{lib}}(t) \tag{9}$$

where

$$C^{\mathrm{rot}}(t) \propto \exp(-t/\tau_{\mathrm{rot}}) \tag{10}$$

using the same jump diffusion model as in deriving Eq. 6.[28]

For the segmental dynamics where no rotations are present, the first fast decay can be described by a generalized Lamb-Mössbauer factor (cf., e.g., [29]) and in that case the amplitude of the slow process is given by

$$A(Q) = \exp\left(-\frac{< u^2 >}{3}Q^2\right) \tag{11}$$

where u is the radius of the "cage" in which the atom vibrates in the fast process. This approach will be used to analyse the amplitudes for the different fitting methods for $S^{seg}(t, Q)$. An independent estimate of $< u^2 >$ can be obtained from the mean squared fluctuation of atomic positions. This can in its turn be obtained by extrapolating the mean squared displacement to $t = 0$ which then yields $2 < u^2 >$

4 Results

4.1 Neutron Scattering

4.1.1 Data reduction

Quasi-elastic spectra from PPO at temperatures T = 240, 270, 290, 300, 325 and 350 K at momentum transfer $Q = 1.1$ Å^{-1} are shown in Fig 1. The

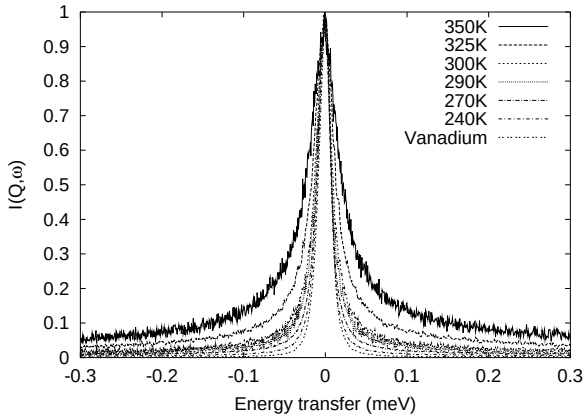

Figure 1: Quasi-elastic neutron scattering spectra from PPO at $Q = 1.1$Å^{-1} T = 240, 270, 290, 300, 325 and 350 K. Dotted line represents the instrument resolution function as obtained from the scattering from a vanadium plate. All spectra have been normalised to unity at E = 0 for the purpose of comparing the shape of the spectra, the slight skewness of the spectra is because the background has not been subtracted.

broadening of the elastic peak with higher temperature is clearly seen. At $T < 290$ K only a small part of the scattering shows broadening beyond the resolution function. Since the chain dynamics at this temperature ($T_g =$ 195K) is very slow, with relaxation times of the order of a few hundred seconds, it is not resolved by the resolution of the instrument. It will therefore appear as purely elastic scattering in the experimental spectrum. We then attribute the small broadenings we see at temperatures below 240 K to the rotational jump diffusion of the methyl side-groups. Above 240 K there is another regime where the whole peak appears to broaden. We attribute this behaviour to the fact that the main α-relaxation becomes faster and moves into the experimental energy window of the spectrometer.

Intermediate scattering functions were thereafter obtained through time-Fourier transform of the experimental data, and the resolution function was subsequently deconvoluted from the spectra through a division by the

time-Fourier transformed resolution. The intermediate scattering function, $S(Q,t)$, for PPO at 1.1Å^{-1} is shown for different temperatures in Fig.2, where the relaxation rate increases with increasing T as expected. The resolution

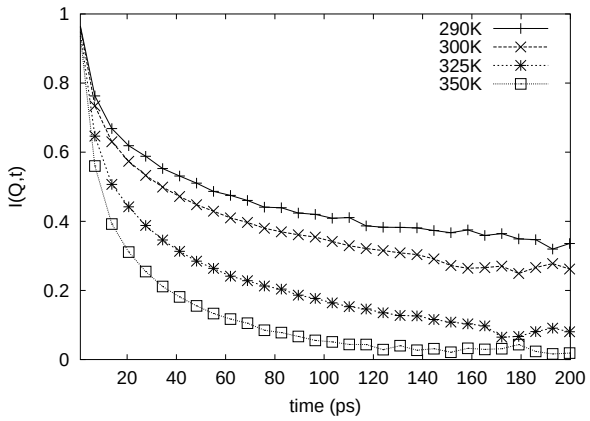

Figure 2: Intermediate scattering function for PPO at Q=1.1Å^{-1} for 290, 300, 325 and 350K. The experimental data, $I(Q,\omega)$, is Fourier transformed and divided by the resolution.

of the instrument sets the long time limit of $I(Q,t)$ and the energy window of the spectrometer sets the short time limit of the measurable Fourier time to be $5 \lesssim t(\text{ps}) \lesssim 200$.

The relaxation behaviour has been analysed in two ways; by using explicit expressions for the methyl group motion and the segmental dynamics, Eq. 2, and, for a comparison, by fitting the intermediate scattering function at each temperature by a stretched exponential function, Eq. 3.

4.1.2 Data analysis

We start at temperatures not far above T_g where the segmental motion is too slow to be detected by the instrument, thus it is assumed that only the methyl group motion is present. The rotational motion relaxation time at 240 and 270 K is then obtained by fitting a Lorentzian function convoluted with the resolution function to the experimental $S(Q,\omega)$, i.e. using the frequency Fourier transform of Eq. 6 with $\beta = 1$, to calculate τ_{rot}. Then for temperatures above 270 K we use τ_{rot}, τ_{seg} and β as adjustable parameters, when we fit the expression in Eq. 2 to the data. The result is presented in Fig. 3.

The $\langle\tau_{\text{seg}}\rangle$ values shown in Fig. 9 display a Q dependence of the relaxation time with $\langle\tau_{\text{seg}}\rangle \propto Q^{-\nu}$, $\nu \approx 2.4 - 3.5$, or $\nu\beta \approx 1.5$.

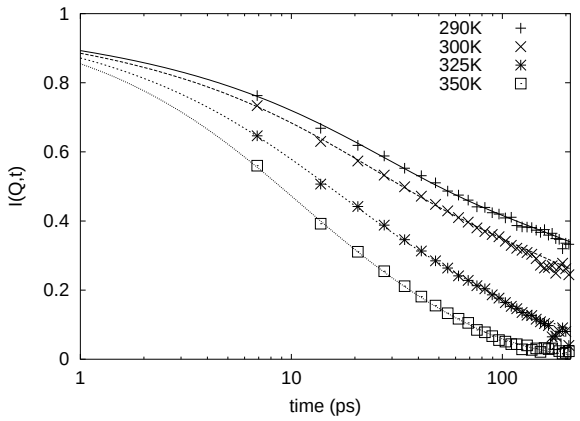

Figure 3: Fits of the model Eq. 2 to the intermediate scattering function at temperatures above 270K an at momentum transfer $Q = 1.1$Å.$^{-1}$ Experimental data are shown as markers and fits as lines. Note that the initial fast decay is not accessible with these experiments and hence the curves do not approach one for small times.

The resulting rotational relaxation times are shown in Fig. 5. The log of the relaxation times agree within 10% with the previous results of Ref. [20], the unphysical increase of the relaxation time in that study is, however, here replaced by the expected decrease, making the present results more reliable.

The activation energy for the rotational jump diffusion can be calculated assuming an Arrhenius behaviour of the relaxation time. This gives a value for the pre-factor $\tau_0 \sim 100$ fs and for $E_A = 13 \pm 3$ kJ/mol,

We summarise the temperature dependence for $\langle \tau \rangle$ in Table 1.

Table 1: Summary of fit parameters from QENS analysis using Eq. 2, time is in ps.

T(K)	τ_{rot}	$\langle \tau_{\mathrm{seg}} \rangle$	β	ν
240	262	$\gg 10^4$		
270	32	$> 10^4$	0.25	
290	20	950	0.38	3.3 ± 0.3
300	23	385	0.42	3.5 ± 0.2
325	9.7	75	0.54	2.8 ± 0.2
350	8.9	30	0.64	2.4 ± 0.1

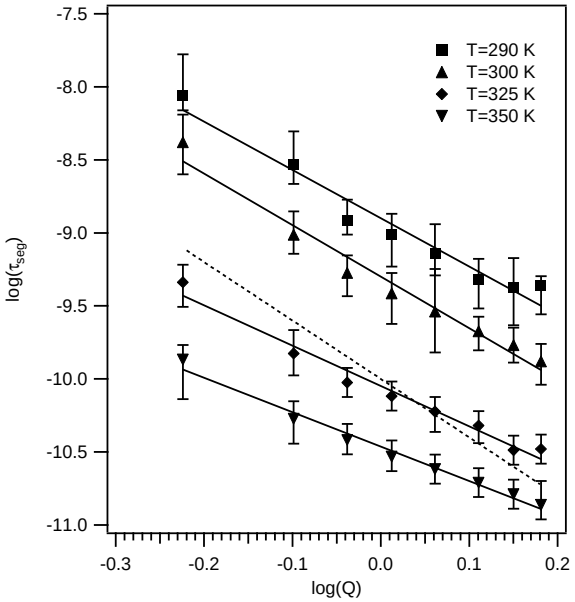

Figure 4: Log-log plot of the segmental motion relaxation time vs. Q. The solid lines are fits to the data of a the power law expression $\tau \propto Q^{-\nu}$ and the broken line corresponds to a dependence $\tau \propto Q^{-4}$ as in a Rouse model. From the plot it is clear that a Rouse model is not applicable to this process.

4.2 Molecular Dynamics

4.2.1 Segmental Dynamics

In the neutron scattering experiments, the dynamics is essentially probed by scattering from the hydrogen atoms whereas in the simulation all atoms are included and can be studied. To characterise the segmental motion in a manner similar to the experimental studies we have calculated the intermediate scattering function at 240 and 300 K for the backbone hydrogen atoms. The obtained scattering functions have then been fitted to stretched exponentials, see Figs. 6 and 7. At 300 K, this fitting has been done over two different intervals using points equally spaced in time. One interval was chosen to 7-180 ps in order to be similar to the experimentally observed interval. The other interval was chosen to cover the part of the simulation where data were most reliable with respect to statistical fluctuations etc. (10-1000 ps). The lower limit was chosen as to avoid any influence of the fast process(es) but is really insignificant to the outcome of the fitting. A fit 7-1000 ps gives an indistinguishable result. For the interval 10-1000 ps fits were either made with the exponent β as a $Q-$dependent fitting parameter or as a fixed value between 0.5 and 0.7 common for all $Q-$values.

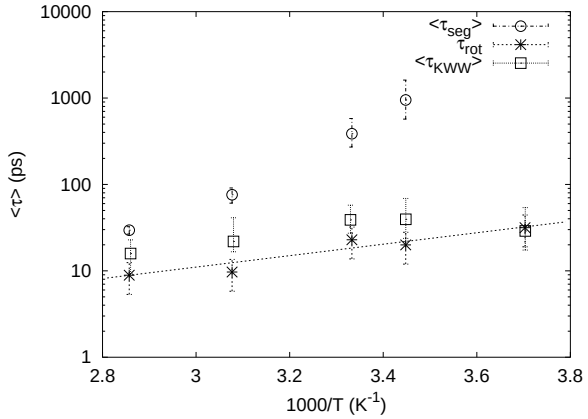

Figure 5: Arrhenius plot of the relaxation times for the segmental $\tau_{\rm seg}$ and rotational $\tau_{\rm rot}$ motion, as obtained from fitting Eq. (2) to the experimental data for $Q = 1.1$ Å^{-1}, together with relaxation times obtained from fitting *only* the KWW function $\tau_{\rm KWW}$ to the data. The$\tau_{\rm KWW}$ only show a very weak temperature dependence whereas the segmental relaxation times show a clearly non-Arrhenius dependence which is an indication of several different barriers being of importance for this relaxation process. The line is a fit of $\tau_{\rm rot}$ to an Arrhenius dependence.

The results over the two fitting intervals with $Q-$dependent β-values are similar except for the lowest Q-values (below 0.8 Å^{-1}, see Fig. 9 where the $\tau(Q)$ from the shorter fitting interval deviate from a straight line. This is an indication that the experimentally accessed interval is close to the lower limit to be be useful. However, the good agreement at higher $Q-$values shows that the experimentally used interval gives relevant results.

Due to the shorter simulation length at 240 K, we only used one fitting interval corresponding to the full simulation length at that temperature. The resulting parameters are given in Table 2.

An analysis of the amplitudes of the slow process is shown in figure 8 where the logarithms of the amplitudes $A(Q)$ are plotted as a function of Q^2. From the slopes we find values of $< u^2 >$ between 0.53 and 0.68 Å^2 for fixed Q-values. Since this is in good agreement with the value obtained from the the mean squared displacement (that is extrapolated to 1.1 Å^2 if the first rapid "in-cage" component is neglected) this gives an indication of the reliability of the the results from the I_s-calculations.

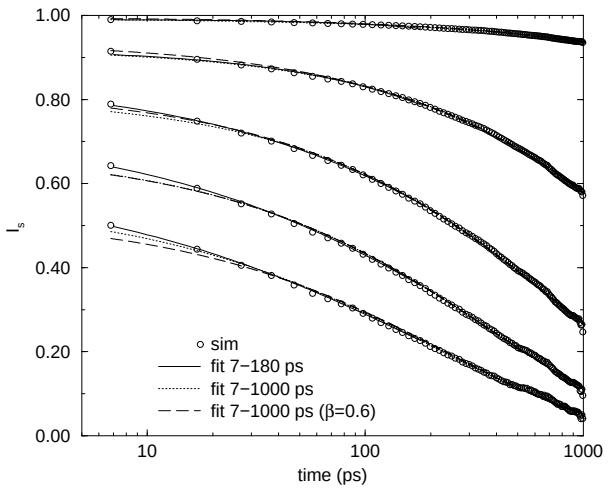

Figure 6: The intermediate scattering function from the simulation at 300K (circles; for clarity only every 100th point is given) as well as stretched exponential fits over different time spans, 7-180 ps (solid curve) and 10-1000 ps (dotted curve). Also given is a fit using a fixed $\beta = 0.6$ (long dashed curve). Curves are given for Q =0.2, 0.6, 1.0, 1.4 and 1.8 Å^{-1}.

4.2.2 Methyl Group Rotation

In the MD simulation one can explicitly follow the dihedral angle ϕ of a methyl group. A typical trajectory is shown in Fig.10. Note that there are well defined "jumps", which corroborates the three site jump model. Also note that there are occasionally some rotations with greater amplitude than 120°. Since the transition time for these jumps is shorter than the resolution of the analysis we cannot differentiate between two one-step jumps with a short intermediate residence time and direct two-step jump. This dynamics affects the S^{vib} which would contain an anomalous Debye-Waller factor caused by these large amplitude jumps.

In total 19696 methyl dihedral jumps were found for the 945 side chain methyl groups during the 1 ns trajectory at 300 K corresponding to jump frequency of 21 GHz. An analysis of the correlation of subsequent jumps as a function of the life time for a certain dihedral state was also made. As expected it shows that two following jumps are mainly uncorrelated with exception for very short life times for which a preference for return jumps was seen. This probably is a consequence of the strict geometric criteria used to determine a certain state which do not necessarily reflect the actual position of the rotational barrier in a given moment due to the influence of the surroundings. For medium lifetimes (1ps $\lesssim t \lesssim$ 100ps) a tiny forward

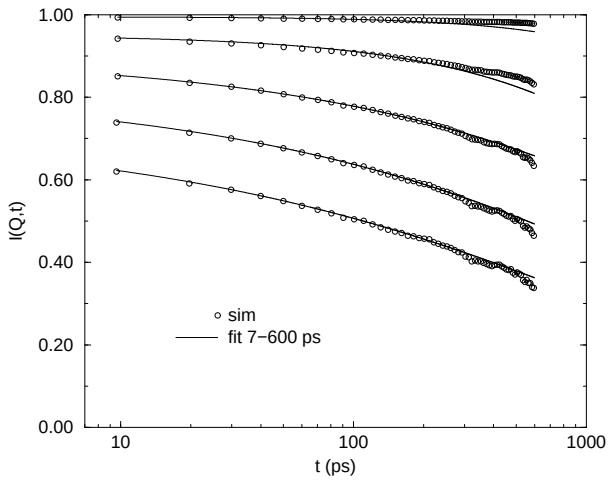

Figure 7: The same as fig.6 but for 240 K. Due to the shorter simulation time only one fitting interval (7-600 ps) was used.

Table 2: Fits of methyl side chain rotational correlation times (simple exponential) and of $\langle\tau\rangle \propto Q^{-\nu}$ for the backbone hydrogens. ν, $\langle\tau\rangle$ and β were taken at $Q = 1.0\text{Å}^{-1}$, relaxation times in ps. The values were obtained from a fit to a stretched exponential for each Q but for $Q > 1\text{Å}^{-1}$, the β-values are nearly independent on Q. At 300 K fits are made within two different time intervals a: 7-180 ps and b: 10-1000 ps.

Group	τ_{rot}	$\langle\tau_{\text{seg}}\rangle$	β
240 K	139		
300 K (a)	40	1700	0.52
300 K (b)	40	1200	0.63
325 K	27		

correlation is found, i.e., a jump in one direction is followed by another jump in the same direction.

Eq. 8 was used to calculate the angular relaxation in Fig. 11. In the inset at short times one can note some oscillations. They are librational (hindered rotational motion) of the CH_3 group. The period of these oscillations is $0.14\pm$ 0.01ps, which corresponds to a frequency of $\nu_{\text{lib}} = 7.2 \pm 0.5$THz (29meV), which is close to the experimental value[9] of 6.8 THz.

At longer times, in the main graph, one notes the relaxational motion of the methyl groups. From this we can calculate the relaxation times τ and stretching parameter β. At 240 K $\tau = 128$ps and $\beta = 0.87$ are obtained, i.e. essentially an exponential decay. This value is in good accordance with the

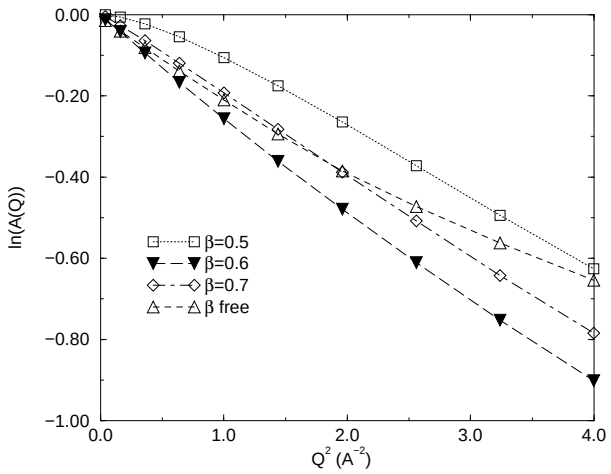

Figure 8: A plot of $\ln(A(Q))$ as a function of Q^2 (Å^{-2}) using different β-values in the fit. The use of fixed $\beta-$values for the fit yields essentially straight lines with slopes corresponding to $< u^2 > \approx 0.7$ Å^2 whereas the result when letting β be a fitting parameter for each Q is a curve approaching $< u^2 > \approx 0.4$ Å^2 for large Q.

experimentally obtained correlation times. If we remake the fit with a forced single exponential decay we obtain $\tau = 139$ps and only a slightly worse fit. Similar results were obtained at the other temperatures and the results for single exponential fits are given in Table 2.

Using these relaxation times the activation energy for the methyl group rotation can be calculated more accurately using the Arrhenius equation

$$\tau^{-1} \propto \exp\left(-\frac{E_A}{k_B T}\right). \tag{12}$$

From the correlation times at different temperatures (see Fig. 12) we then obtain $E_A = 12.6 \pm 0.2$kJmol^{-1} which is close to our previous estimate. This value can be compared to the experimentally obtained value $E_A = 13 \pm 3$ kJ/mol (see Sec.4.1.2) and we find that there is an excellent agreement between the simulated and experimental results.

5 Discussion

Even though we have used the simplest model conceivable for the segmental and rotational motion, it describes both the experimental and simulated data well. It was clearly demonstrated how the non-physical results, when using

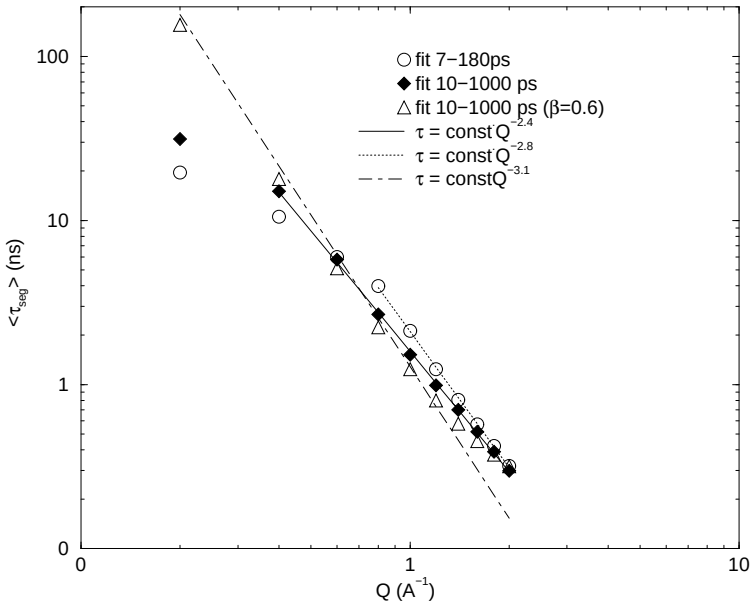

Figure 9: a) The average relaxation time $\langle\tau\rangle$ from the simulation at 300K as a function of the momentum transfer Q. Two fits to the curves in figure 6 are given over different intervals: 7-180 ps, corresponding to the experimental data and 10-1000 ps, an interval covering the most reliable data from the simulation. For each of these curves a fit of $\tau \propto Q^{-\nu}$ is given where all parameters in the KWW-expression were fitted. Whereas the fit over 7-180 ps is somewhat better in reproducing the experimental results at short times, it is worse at longer times

only a stretched relaxor, is transformed into physically sensible results when a full model including simultaneously rotations and segmental motions was used.

The MD study with its wider time range has made it possible to check that the rather narrow time range available in the QENS experiment does not seriously influence the results regarding the segmental motion. This was done by fitting the MD results using different time ranges, corresponding to changing the resolution of the neutron scattering experiment. Figure 9 shows that a small time window (open circles) used for the QENS experiment can give a slightly different exponent ν, as compared to a larger time window (filled diamonds). However, the fitting of the results to a stretched exponential is not unambigous and the use of a fixed $\beta = 0.6$ (open triangles) (with the longer time window) yields somewhat different results with a slope slightly larger than 3.

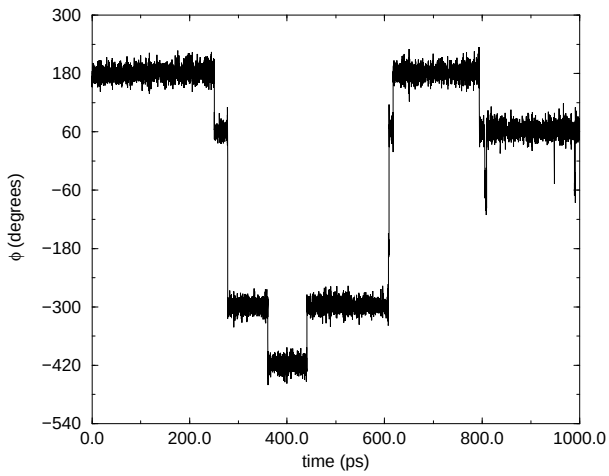

Figure 10: A typical trajectory for the CH_3 dihedral angle.

The obtained values of $\tau_{\rm seg}$ agree well with previous results from neutron scattering, and qualitatively with previously reported results for the α-relaxation obtained from photon correlation spectroscopy (PCS) and impulsive stimulated light scattering (ISS). [25, 30, 31] The exponent ν (see Eq. 4 is found to be between 2.4 and 3.5 for the whole Q range contradicting the cross-over to a Gaussian type of dependence, with $\nu = 2/\beta$, for the relaxation rate, at the first peak of the structure factor as reported in e.g. Ref. [32]. It should however be noted that preliminary spin echo data[33] show that the relaxation rate for PPO with $Q \lesssim 0.3\text{Å}^{-1}$ is compatible with $\nu = 2/\beta$. It could be that the transition in PPO takes place at slightly lower Q values than found in previously studied polymers.

According to the MD results, the rotational correlation function of the methyl group decays essentially exponentially. A small deviation from exponentiallity is, however, found such that β is slightly lower than one. This could be due to the slight correlation of successive jumps, as described earlier. A more prominent reason is, however, the fact that the different methyl groups are situated in slightly different surroundings which means that the correlation function is actually averaged over several different groups with different correlation times. This can also be seen from the correlation functions for different methyl groups which differ on the 1 ns time scale of the simulation. The fact that we can use single relaxation time for the rotation is probably related to the fact that, as pointed out in Ref.[8, 12], the width of the distribution of barriers tends to be similar for many polymers and in our case of a high activation energy the spread is of minor importance. Moreover, the width of the distribution of energy barriers is independent of temperature

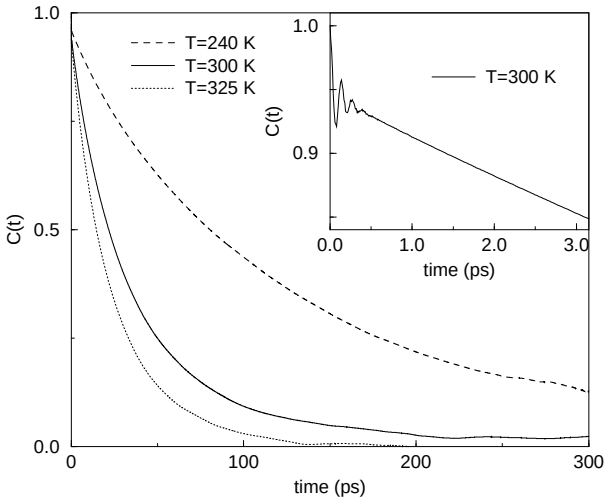

Figure 11: The relaxational behaviour of the CH_3 group. In the inset the short time librational motion is shown.

which leads to a narrowing, as temperature increase, of the distribution of relaxation frequencies, which is what is measured. It is, however, clear from the simulation that there is a distribution even though the effect is hardly seen in the experimental results. It is possible that, if experiments where carried out at temperature below the glass-transition, we would have to consider a distribution. The activation energy for the rotational jump diffusion assuming an Arrhenius behaviour of the relaxation time that was calculated from the neutron scattering data in Sec.4.1.1 is of the same order as the value calculated from the simulation in Sec.4.2, The value of $\tau_0 \sim 100$ fs, from the NS experiment is of the same order of magnitude as the value of $\tau_0 \sim 150$ fs from the libration in the simulation which is again a corroboration of both the experimental results as well as the MD model.

The activation energy in qualitative agreement with earlier reported value of E_A=16 kJ/mol.[6] Even though the influence from the multiple scattering is relatively stronger for the faster (broader) component of the relaxation, one can expect a smaller effect on properties derived from differences at varying temperature, since to a first approximation the multiple scattering introduces a constant, temperature independent level shift of the relaxation time. New experiments are planned to confirm the present analysis and even if the single exponential description works well, we plan in the future to expand the study with a distribution of relaxation times, by making a low temperature study, to determine if it is possible to deduce a distribution of relaxation times.

The dynamics of the MD simulation is somewhat slower than the mea-

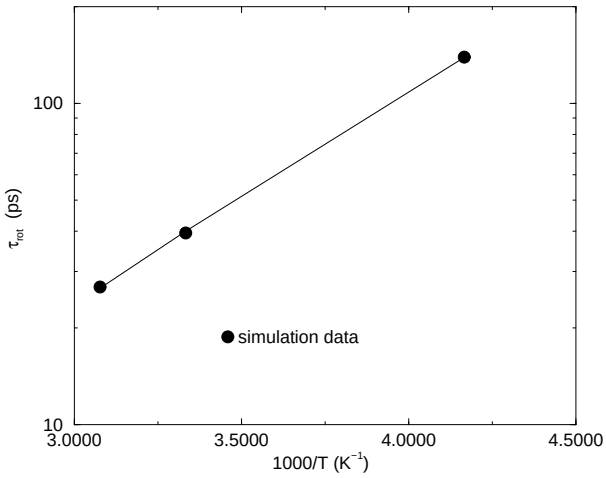

Figure 12: An Arrhenius plot of the logarithm of the rotational correlation times for the side chain methyl dihedrals (as obtained from the simple exponential fits, cf. text and Table 2).

sured one. One reason for this could be the modelling of electrostatic interactions where charges were obtained from fitting to the electric field outside a series of conformers[17]. The effective dipole moments obtained in this way are a few percent higher than the originally calculated ones. This means that the partial point charges obtained in this way are in part effective charges which should have been modelled as polarisabilities to make a more correct model. Another reason could be the fact that the errors in the measured values of the rotation times, if influenced by multiple scattering, would make the measured values seem faster than they are. A small increase of the effective fixed charges will lead to a much slower dynamics than if the same dipole increase was made by means of a polarisability (see e.g. Ref. [34]). The dynamic properties are generally much more sensitive to the accuracy of the force field than static properties and hence a forcefield that yields practically perfect static properties could show small deviations in the dynamic properties. In the light of this the agreement between the experimental and simulated results for the dynamics should be regarded as representing the real system in a *very* good way.

It should again be noted that without fitting simultaneously the segmental and rotational dynamics it is not possible to get a physical interpretation of results.

6 Conclusion

It is well known that molecular dynamics simulations and neutron scattering data are useful, necessary complementary tools to rationalise the intricate dynamics of polymer systems. MD simulations performed with quantum chemically determined all-atom potential which is more complicated than a united-atom force-field in which the heavy atoms and hydrogens are united to one atom increase the simulation time by about a factor of six. This is however necessary to be able to calculate neutron scattering data which are dominated by the contributions from the hydrogen atoms and make it possible to study methyl group dynamics.

We have, without resorting to selective deuteration, separated contributions from segmental dynamics and methyl side-group rotations in QENS spectra from PPO by using a simple model. This separation is important to get physically realistic results for the dynamics in the regime where we have segmental relaxations.

The temperature dependence of the segmental relaxation time is in accordance with results from earlier work on PPO. The fact that the distribution of relaxation times is so narrow that we can use a delta function at these temperatures does not contradict the hypothesis of a constant width of the activation energy barrier distribution. The relaxor rate distribution, which is measured, does become more narrow with increasing temperature, if the distribution in energy barriers is constant. A study at lower temperature would make it possible to determine a distribution, albeit narrow, of relaxation times.

The Q-dependence of the α-relaxation time does not show the cross-over to $\nu = 2/\beta$ expected for a homogeneous, intrinsically stretched, segmental relaxation, but rather a $\nu \sim 2$ dependence over the whole Q range investigated. This result merits further study as the Q range available in this work was limited and indeed, preliminary NSE results indicate that there might be a cross-over around 0.3Å^{-1}.

By using MD simulations it is possible to get a clearer picture of the contributions from different groups to the obtained scattering function and thus to confirm the validity of the model presented. It was thus possible to confirm that the rotational relaxation of the methyl group was essentially exponential with only a small heterogeneous stretching.

Since the MD simulations covered a six times wider time range than the experiments it was possible to show that the obtained results are rather insensitive to the actual fitting range. However the exact vaules of the exponents etc. are sensitive to the fitting procedure chosen and hence some care should be exercised when comparing different results. Since the simulation results

do not contain experimental artefacts like multiple scattering, the fact that the $Q-$dependence of the relaxation was very similar in the simulations and in the experiments which is a strong indication that the found value of $\nu \sim 3$ is the correct one in this Q range ($0.45 < Q/\text{Å} < 1.85$) for the PPO system.

Acknowledgements

Beam-time at ISIS and financial support of the Swedish NFR are gratefully acknowledged.

References

[1] W. Paul, G.D. Smith, D.Y. Yoon, B. Farago, S. Rathgeber, A. Zirkel, L. Willner, and D. Richter, Phys. Rev. Lett. **80**, 2346 (1998).

[2] J. Colmenero, A. Arbe, G. Coddens, B. Frick, C. Mijangos, and H. Reinecke, Phys. Rev. Lett. **78**, 1928 (1997).

[3] A. Arbe, J. Colmenero, M. Monkenbusch, and D. Richter, Phys. Rev. Lett **81**, 590 (1998).

[4] P. Schleger, B. Farago, C. Lartigue, A. Kollmar, and D. Richter, Phys. Rev. Lett. **81**, 124 (1998).

[5] G. Allen, J.S. Higgins, A. Maconnachi, and R.E. Ghosh, J. Chem. Soc., Faraday Trans. II **78**, 2117 (1982).

[6] G. Allen and J.S. Higgins, Macromolecules **10**, 1006 (1977).

[7] J. Colmenero and A. Arbe, Phys. Rev. B **57**, 13508 (1998).

[8] R. Mukhopadhyay, A. Alegría, and J. Colmenero, Macromolecules **31**, 3985 (1998).

[9] J.S. Higgins, G. Allen, and P.N. Brier, Polymer **13**, 157 (1972).

[10] V. Arrighi and J.S. Higgins, Physica B **226**, 1 (1996).

[11] B. Gabrys, J.S. Higgins, K.T. Ma, and J.E. Roots, Macromolecules **17**, 560 (1984).

[12] A. Chahid, Alegría, and J. Colmenero, Macromolecules **27**, 3282 (1994).

[13] J. Colmenero, R. Mukhopadhyay, A. Alegría, and B. Frick, Phys. Rev. Lett. **80**, 2350 (1998).

[14] F. Alvarez, A. Arbe, and J. Comenero, Chem. Phys. **261**, 47 (2000).

[15] K. Karatasos, J.-P Ryckaert, R. Ricciardi, and Lauprêtre, Macromolecules **35**, 1451 (2002).

[16] P. Carlsson, J. Swensson, L. Börjesson, L.M. Torell, R.L. McGreevy, and W.S. Howells, J. Chem. Phys. **109**, 8719 (1998).

[17] G.D. Smith, O. Borodin, and D. Bedrov, J. Phys. Chem **A102**, 10318 (1998).

[18] P. Ahlström, O. Borodin, G. Wahnström, E.J.W. Wensink, P. Carlsson, and G.D. Smith, J. Chem. Phys. **112**, 10669 (2000).

[19] Mattias Slabanja and Göran Wahnström, Chem. Phys. Lett. **324**, 593 (2001).

[20] D. Andersson, P. Carlsson, D. Engberg, L.M. Torell, L. Börjesson, R.L. McGreevy, and W.S. Howells, Physica B **266**, 126 (1999).

[21] D. Engberg, J Schüller, B. Strube, A.P Sokolov, and L. M. Torell, Polymer **40**, 4755 (1999).

[22] Peter Ahlström, Göran Wahnström, Patrik Carlsson, Staffan Schantz, Alexander Brodin, Frans Mauer, and Lena M Torell, Philos. Mag. B **77**, 699 (1998).

[23] W.F. van Gunsteren and H.J.C. Berendsen, *Gromos manual* (University of Groningen, Gronigen, 1987).

[24] H. J. C. Berendsen, D. van der Spoel, and R. van Drunen, Comp. Phys. Comm. 43 (1995).

[25] R. Bergman, L. Börjesson, L. M. Torell, and A. Fontana, Phys. Rev. B **56**, 11619 (1997).

[26] D. Richter, M. Monkenbusch, J. Arbe, A. Colmenero, B. Farago, and R. Faust, J. Phys: Condens. Matter **11**, A297 (1999).

[27] A. Arbe, J. Colmenero, F. Alvarez, M. Monkenbuch, D. Richter, B. Farago, and B. Frick, Physical Review E **67**, 051802 (2003).

[28] M. Bée, *Quasi-elastic neutron scattering* (Adam Hilger, Bristol, 1988).

[29] S.-H. Chen, P. Gallo, F. Sciortino, and P. Tartaglia, Phys.Rev.E **56**, 4231 (1997).

[30] P. Carlsson, in *Slow dynamics in complex systems*, edited by M. Tokuyama and I. Oppenheim (Springer-Verlag, New York, 1999).

[31] A.R. Duggal and K.A. Nelson, J. Chem. Phys **94**, 7677 (1991).

[32] J. Colmenero, F. Alvarez, and A. Arbe, Phys. Rev. E **65**, 41804 (2002).

[33] D. Andersson, private comunication.

[34] P. Ahlström, A. Wallqvist, S. Engström, and B. Jönsson, Mol. Phys. **68**, 563 (1989).